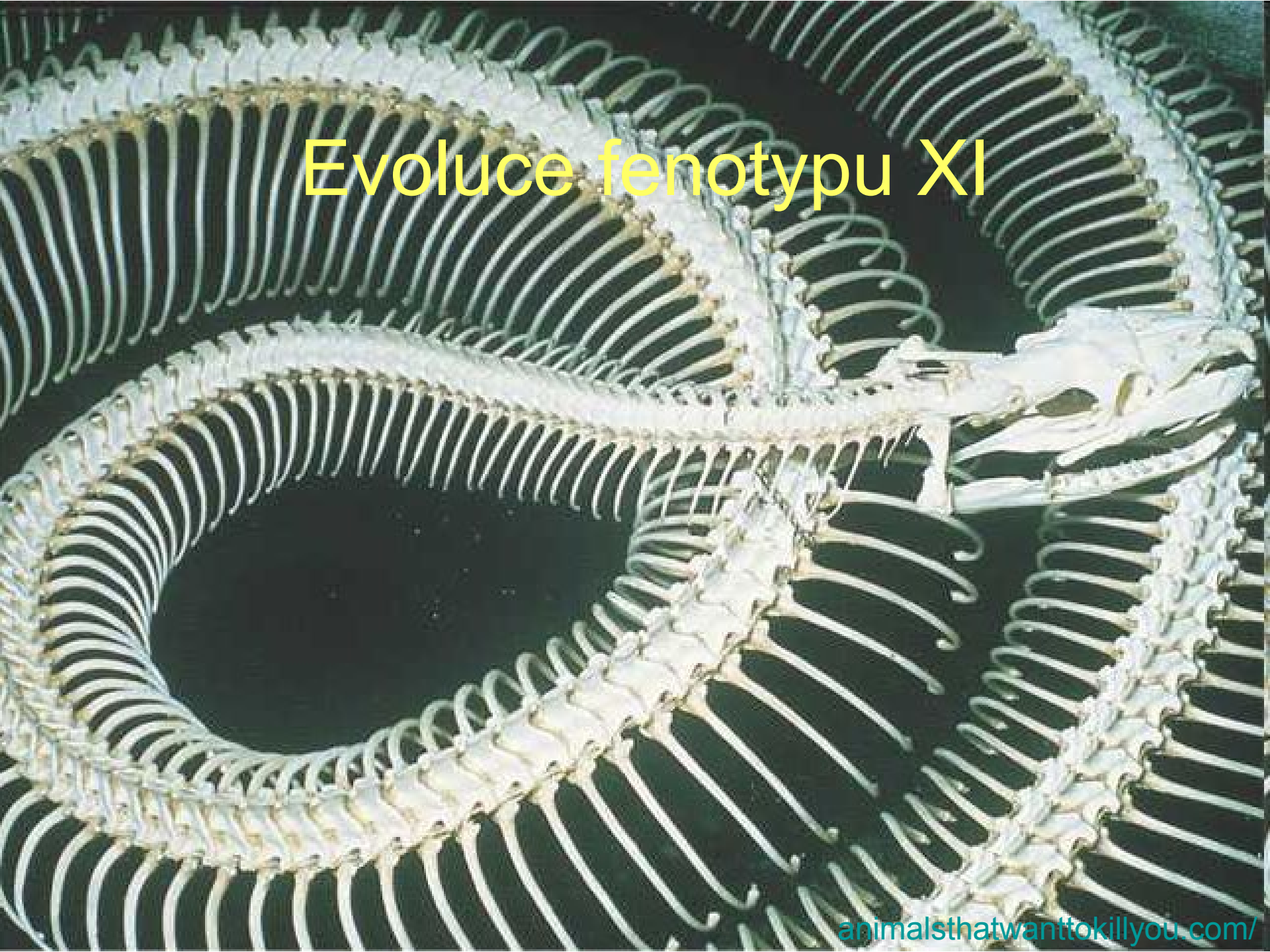
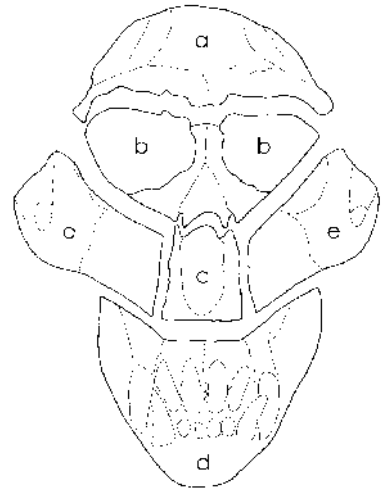
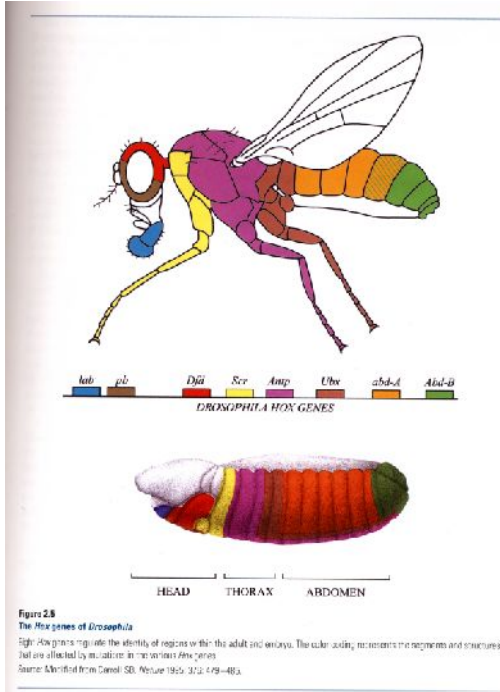


Evolve fenotypu XI



# Tělní plán

- modularita, integrace
- seriální homologie – Willistonovo pravidlo



**Fig. 4.5.** Modularity, plasticity, and integration in the primate face. Skeletal subunits a-e are associated with the functional components of the face. Each lettered component is a developmentally and functionally related unit, and the facial components are highly integrated even while each is semi independently variable. Integration of functionally and developmentally semi-independent components is likely facilitated by the plasticity of contiguous subunits of bone during growth. After Cheverud (1982)

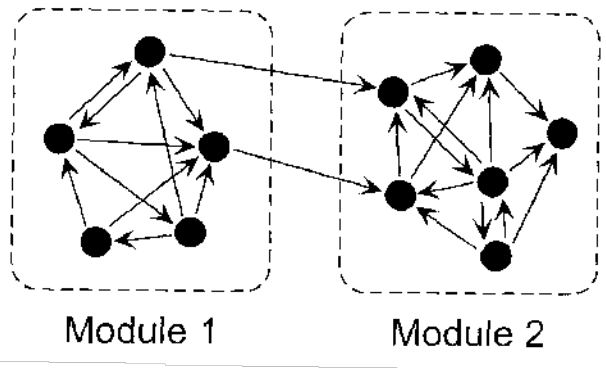


**Figure 10.1** Definition of modules by developmental interactions. Component parts within modules are interconnected by many interactions, whereas there are fewer interactions between modules.

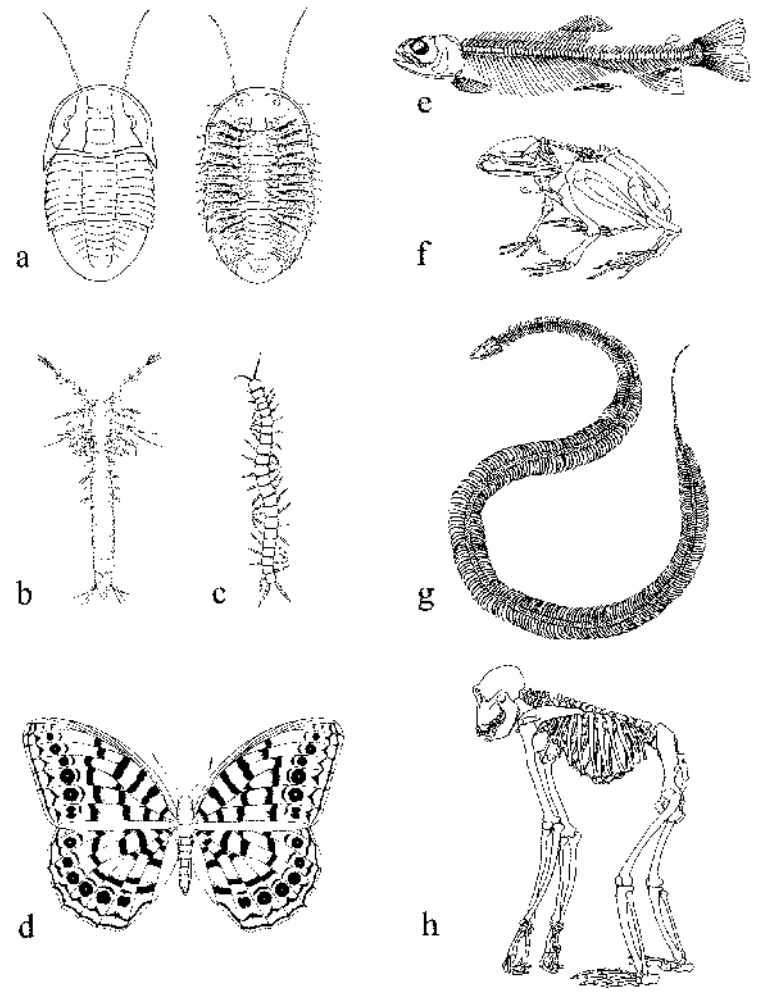


**Figure 1.6**  
**Meristic differences among arthropods and among vertebrates**  
Among arthropods such as the trilobite (a), crustacean (b), centipede (c), and insect (d) the number of body segments differs, as does the diversity of segment morphology. Among vertebrates, the number of vertebrae and associated processes differs considerably between a fish (e), frog (f), python (g), and chimpanzee (h).

# Principy makroevolučních změn fenotypu: Fúze a heterotopie

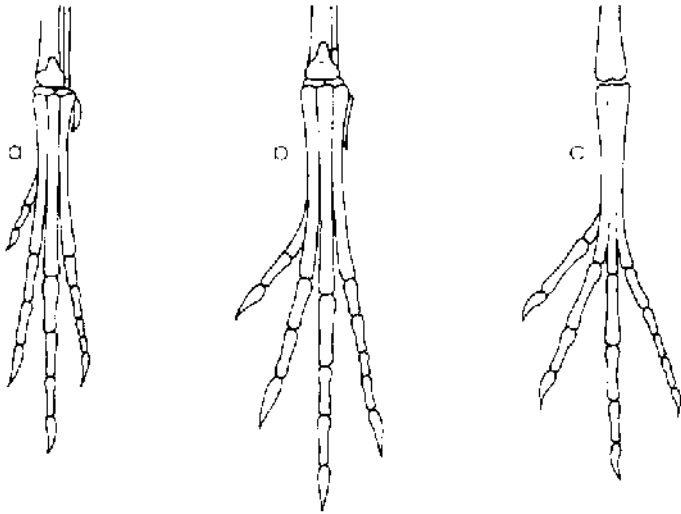


**Fig. 9.2.** Novelty by fusion. The five metatarsal bones in the feet of reptiles were reduced to three in bipedal archosaurs (a), partially fused in *Archaeopteryx* (b), and highly fused in modern birds (c). Based on Frazzetta (1975), Ostrom (1976), and Hall (1984).

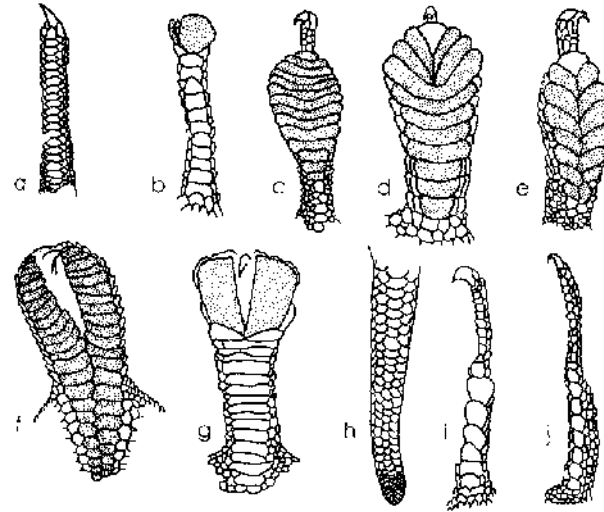


**Fig. 14.2.** Heterotopic variation in the expression of epidermal pads on the feet and tail in different species of geckos. Epidermal pads (shaded) are specialized scales with a velvety covering of fine hairs that facilitate climbing. (a) Simple fourth toe of *Coleonyx variegatus* without pads. (b–g) Patterns of enlarged, padded scales in the fourth toe of different species. (h) Padded scales at the tip of the tail of *Lygodactylus picturatus*, which has toe pads similar to those in (e). (i) Enlarged, unpadded proximal digital scales in fourth toe of *Gonatodes humeralis*. (j) Small, unpadded proximal scales in fourth toe of *Gonatode fuscus*. After Underwood (1954).



# Principy makroevolučních změn fenotypu: Duplikace a divergence funkcí, koopce

## From genome to “venome”: Molecular origin and evolution of the snake venom proteome inferred from phylogenetic analysis of toxin sequences and related body proteins

Bryan G. Fry

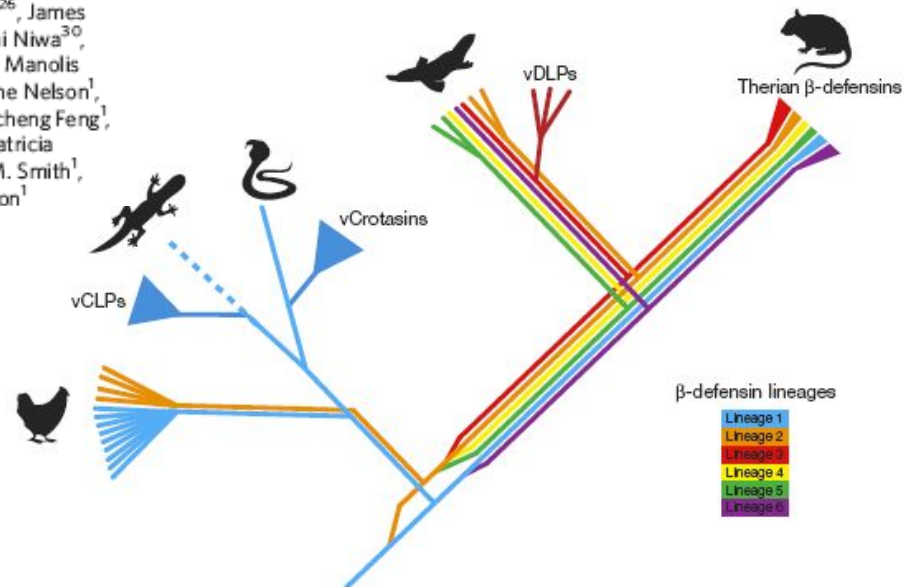
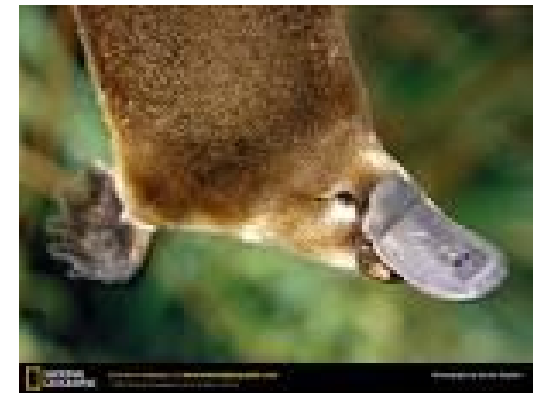


**Table 4.** Bioactivities of the ancestral proteins

Ancestral protein	Activity
Acetylcholinesterase	Rapidly hydrolyses choline released into the synapse, resulting in less neurotransmitter available for neuromuscular control.
ADAM	ADAM 7 - noncatalytic metalloproteinase-like proteins; ADAM 28 - enzymatic cleavage of the extracellular matrix.
BNP	Lowering of blood pressure mediated by the relaxation of vascular smooth muscle subsequent by binding the GC-A receptor and stimulating the intracellular production of cGMP.
C3	Central to both classical and alternative complement pathways.
CNP-BPP	BPP - Indirectly cause hyperpermeability of blood vessels and hypotension by inhibiting the activity of the angiotensin-converting enzyme and enhances the action of bradykinin by inhibiting the kinases that inactivate; CNP - Lowers blood pressure mediated by the relaxation of vascular smooth muscle by binding the GC-B receptor and stimulating the intracellular production of cGMP.
CRISP	Specific actions largely uncharacterized.
Crotasin	Unknown; related $\beta$ defensin peptides have an antimicrobial activity.
E/M/N Cystatin	Inhibit cysteine proteases such as the cathepsins B, L, and S.
Endothelin-3	Potently vasoconstrictive, modulating the contraction of cardiac and smooth muscle.
Factor V	Blood cofactors that participate with factor Xa to activate prothrombin to thrombin.
Factor X	Vitamin K-dependent glycoproteins that convert prothrombin to thrombin in the presence of factor Va, calcium, and phospholipid during blood clotting.
Kallikrein (glandular/tissue)	Release kinins from circulatory kininogen.
Kunitz	Inhibit a diverse array of serine proteinases.
L-amino oxidase	Induce apoptosis in cells by two distinct mechanisms; one rapid and mediated by $H_2O_2$ , the other delayed and mediated by deprivation of L-lysine.
Lectin	Hemagglutination activity.
LYNX/SLUR	Bind to the $\alpha 7$ nicotinic acetylcholine receptor.
$\beta$ Nerve growth factors	Stimulate division and differentiation of sympathetic and embryonic sensory neurons.
PLA <sub>2</sub> (type IB)	Release arachidonic acid from the sn-2 position of the plasma membrane phospholipids.
PLA <sub>2</sub> (type IIA)	Release arachidonic acid from the sn-2 position of the plasma membrane phospholipids, involved in inflammatory processes and diseases, such as rheumatoid arthritis and asthma.
Prokineticin 2	Potent constriction of intestinal smooth muscle and induction hyperalgesia.
SPRY	Largely uncharacterized.
VEGF	Increase the permeability of the vascular bed.
Whey acidic peptide	Inhibit leukoproteinases.

# Genome analysis of the platypus reveals unique signatures of evolution

Wesley C. Warren<sup>1</sup>, LaDeana W. Hillier<sup>1</sup>, Jennifer A. Marshall Graves<sup>2</sup>, Ewan Birney<sup>3</sup>, Chris P. Ponting<sup>4</sup>, Frank Grützner<sup>5</sup>, Katherine Belov<sup>6</sup>, Webb Miller<sup>7</sup>, Laura Clarke<sup>8</sup>, Asif T. Chinwalla<sup>1</sup>, Shiaw-Pyng Yang<sup>1</sup>, Andreas Heger<sup>4</sup>, Devin P. Locke<sup>1</sup>, Pat Miethke<sup>2</sup>, Paul D. Waters<sup>2</sup>, Frédéric Veyrunes<sup>2,9</sup>, Lucinda Fulton<sup>1</sup>, Bob Fulton<sup>1</sup>, Tina Graves<sup>1</sup>, John Wallis<sup>1</sup>, Xose S. Puente<sup>10</sup>, Carlos López-Otin<sup>10</sup>, Gonzalo R. Ordóñez<sup>10</sup>, Evan E. Eichler<sup>11</sup>, Lin Chen<sup>11</sup>, Ze Cheng<sup>11</sup>, Janine E. Deakin<sup>2</sup>, Amber Alsop<sup>2</sup>, Katherine Thompson<sup>2</sup>, Patrick Kirby<sup>2</sup>, Anthony T. Papenfuss<sup>12</sup>, Matthew J. Wakefield<sup>12</sup>, Tsviya Olender<sup>13</sup>, Doron Lancet<sup>13</sup>, Gavin A. Huttley<sup>14</sup>, Arian F. A. Smit<sup>15</sup>, Andrew Pask<sup>16</sup>, Peter Temple-Smith<sup>16,17</sup>, Mark A. Batzer<sup>18</sup>, Jerilyn A. Walker<sup>18</sup>, Miriam K. Konkel<sup>18</sup>, Robert S. Harris<sup>7</sup>, Camilla M. Whittington<sup>6</sup>, Emily S. W. Wong<sup>6</sup>, Neil J. Gemmell<sup>19</sup>, Emmanuel Buschiazzi<sup>19</sup>, Iris M. Vargas Jentzsch<sup>19</sup>, Angelika Merkel<sup>19</sup>, Juergen Schmitz<sup>20</sup>, Anja Zemann<sup>20</sup>, Gennady Churakov<sup>20</sup>, Jan Ole Kriegs<sup>20</sup>, Juergen Brosius<sup>20</sup>, Elizabeth P. Murchison<sup>21</sup>, Ravi Sachidanandam<sup>21</sup>, Carly Smith<sup>21</sup>, Gregory J. Hannon<sup>21</sup>, Enkhjargal Tsend-Ayush<sup>5</sup>, Daniel McMillan<sup>2</sup>, Rosalind Attenborough<sup>2</sup>, Willem Rens<sup>9</sup>, Malcolm Ferguson-Smith<sup>9</sup>, Christophe M. Lefèvre<sup>22,23</sup>, Julie A. Sharp<sup>23</sup>, Kevin R. Nicholas<sup>23</sup>, David A. Ray<sup>24</sup>, Michael Kube<sup>25</sup>, Richard Reinhardt<sup>25</sup>, Thomas H. Pringle<sup>26</sup>, James Taylor<sup>27</sup>, Russell C. Jones<sup>28</sup>, Brett Nixon<sup>28</sup>, Jean-Louis Dacheux<sup>29</sup>, Hitoshi Niwa<sup>30</sup>, Yoko Sekita<sup>30</sup>, Xiaoqi Huang<sup>31</sup>, Alexander Stark<sup>32</sup>, Pouya Kheradpour<sup>32</sup>, Manolis Kellis<sup>32</sup>, Paul Flicek<sup>3</sup>, Yuan Chen<sup>3</sup>, Caleb Webber<sup>4</sup>, Ross Hardison<sup>7</sup>, Joanne Nelson<sup>1</sup>, Kym Hallsworth-Pepin<sup>1</sup>, Kim Delehaunty<sup>1</sup>, Chris Markovic<sup>1</sup>, Pat Mink<sup>1</sup>, Yucheng Feng<sup>1</sup>, Colin Kremitzki<sup>1</sup>, Makedonka Mitreva<sup>1</sup>, Jarret Glasscock<sup>1</sup>, Todd Wylie<sup>1</sup>, Patricia Wohldmann<sup>1</sup>, Prathapan Thiru<sup>1</sup>, Michael N. Nhan<sup>1</sup>, Craig S. Pohl<sup>1</sup>, Scott M. Smith<sup>1</sup>, Shunfenz Hou<sup>1</sup>, Marilyn B. Renfree<sup>16</sup>, Elaine R. Mardis<sup>1</sup> & Richard K. Wilson<sup>1</sup>



NATURE | Vol 453 | 8 May 2008

**Figure 4 | The evolution of  $\beta$ -defensin peptides in platypus venom gland.** The diagram illustrates separate gene duplications in different parts of the phylogeny for platypus venom defensin-like peptides (vDLPs), for lizard

venom crotonamine-like peptides (vCPLs) and for snake venom crotamines. These venom proteins have thus been co-opted from pre-existing non-toxin homologues independently in platypus and in lizards and snakes<sup>48</sup>.

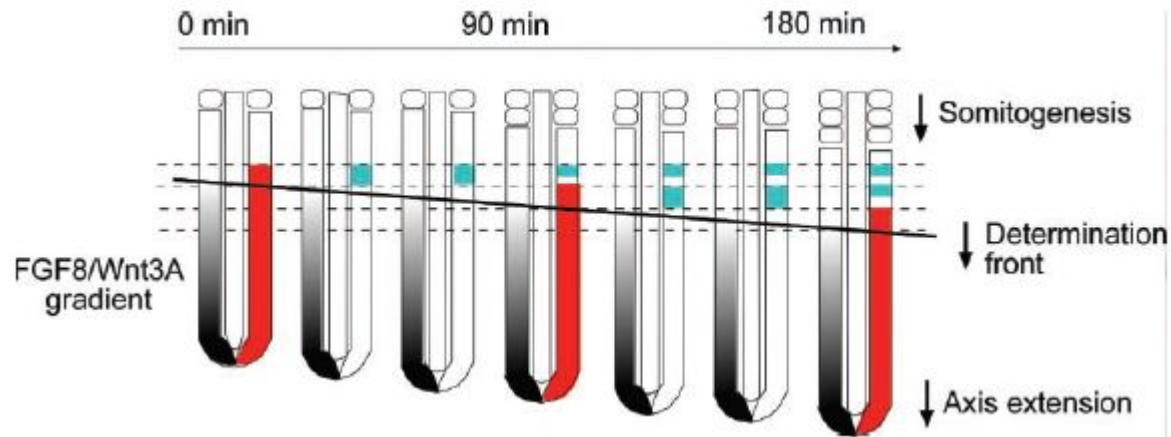
# Principy makroevolučních změn fenotypu: Duplikace

- změny počtu obratlů

## The Segmentation Clock: Converting Embryonic Time into Spatial Pattern

Olivier Pourquié

18 JULY 2003 VOL 301 SCIENCE



# Principy makroevolučních změn fenotypu: Duplikace

- nestabilita a fenotypová plasticita počtu obratlů (Jordanovo pravidlo)

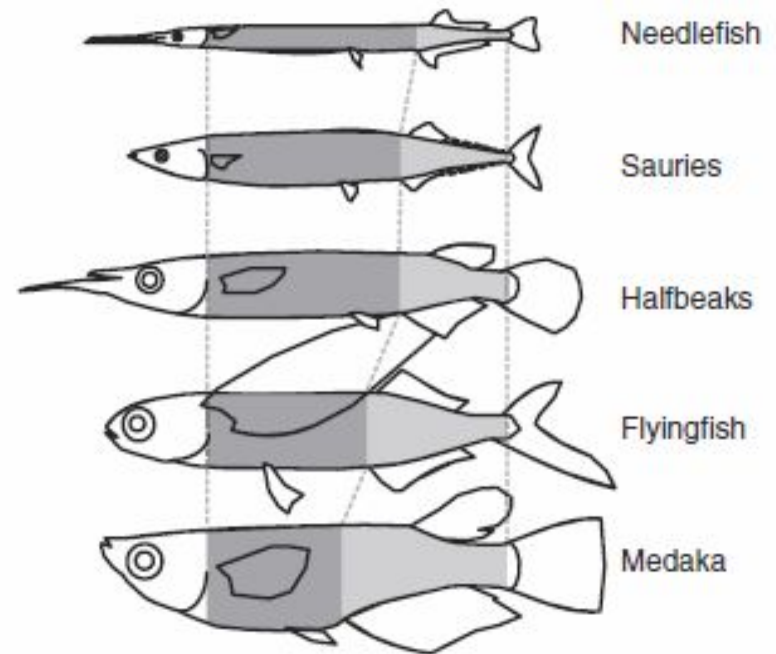
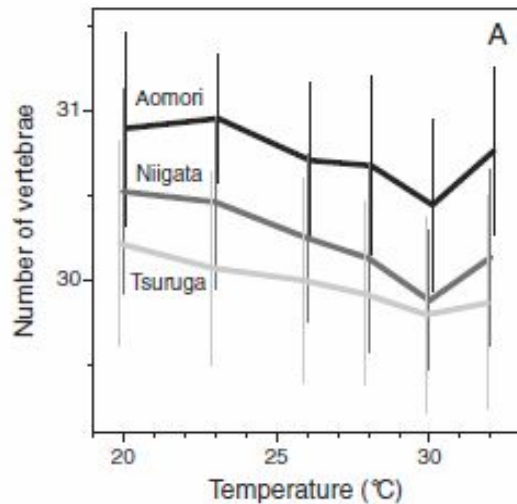


**Figure 1.** Axial diversification of Beloniformes. Dark and light grey portions indicate abdominal and caudal regions, respectively.

*Biological Journal of the Linnean Society*, 2009, **96**, 856–866. With 5 figures

**Latitudinal variation in axial patterning of the medaka (Actinopterygii: Adrianichthyidae): Jordan's rule is substantiated by genetic variation in abdominal vertebral number**

KAZUNORI YAMAHIRA\* and TAKESHI NISHIDA†



# Principy makroevolučních změn fenotypu: Duplikace

- homeotická mutace? Změna načasování osifikace?

Evolutionary novelties: the making and breaking of pleiotropic constraints

Frietson Galis<sup>1,\*</sup>, and Johan A. J. Metz<sup>\*,†</sup>  
*Integrative and Comparative Biology*, volume 47, number 3, pp. 409–419



## Skeletal development in sloths and the evolution of mammalian vertebral patterning

Lionel Hautier<sup>a,1</sup>, Vera Weisbecker<sup>b</sup>, Marcelo R. Sánchez-Villagra<sup>c</sup>, Anjali Goswami<sup>d</sup>, and Robert J. Asher<sup>a,1</sup>

[www.pnas.org/cgi/doi/10.1073/pnas.1010335107](http://www.pnas.org/cgi/doi/10.1073/pnas.1010335107)

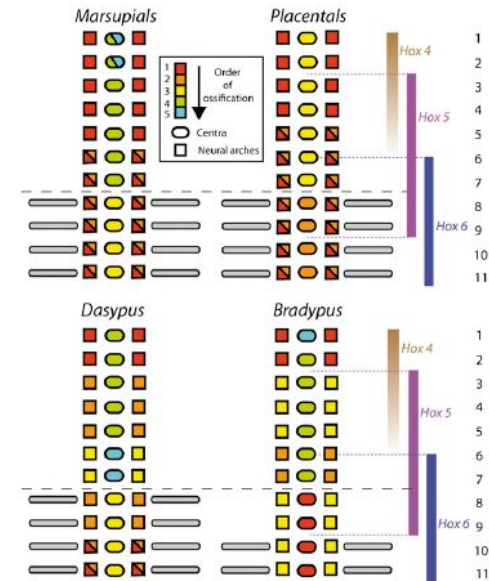
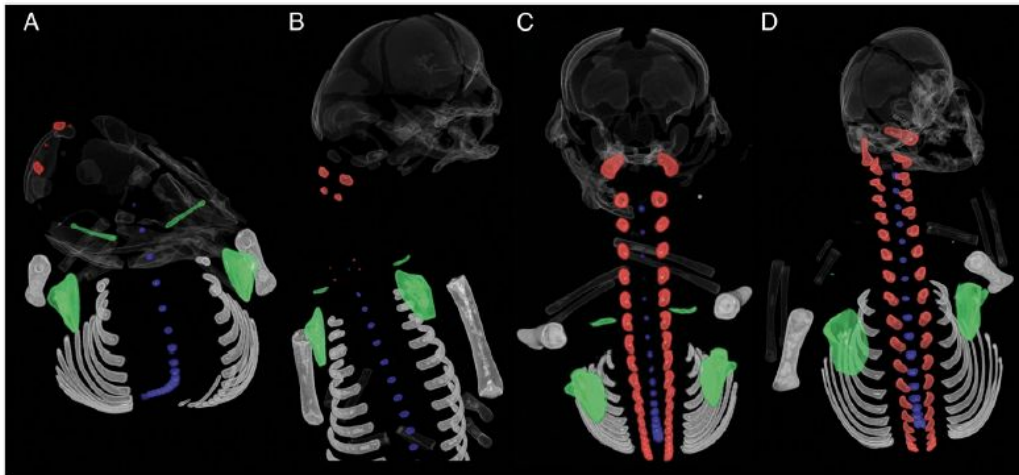
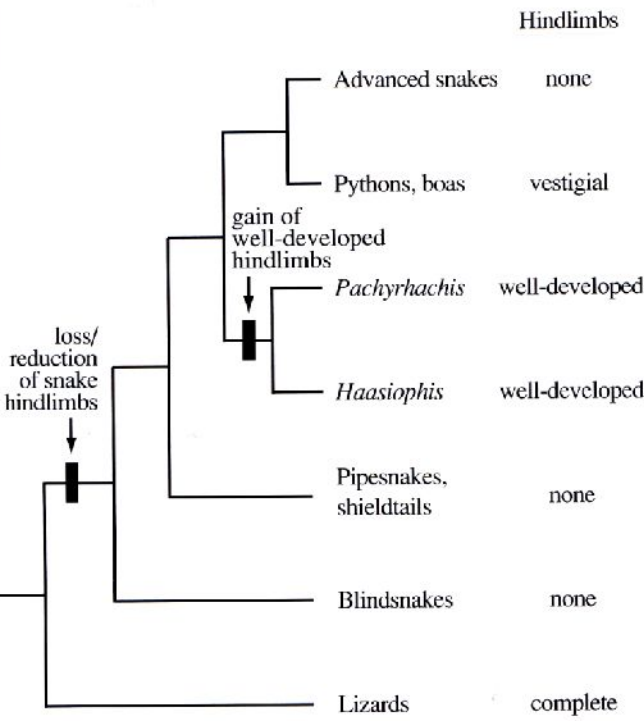
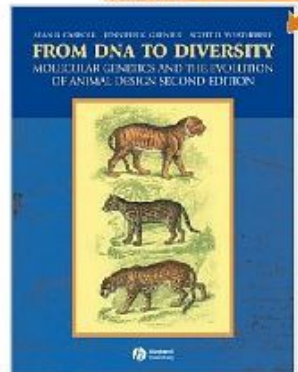


Fig. 4. Summary of ossification sequences in the first 11 mammalian vertebral elements. For each taxon, circles indicate centra, and squares indicate left and right neural arches. Colors represent the order of ossification. Hox expression boundaries in the mouse [redrawn from figure 5 in Wellik (25)] and vertebral segment identity are shown at right. Note the conserved timing of V7 centrum ossification across mammals, including sloths, and the overlap in *Hox5-6* expression in the V6–V9 region of the sloth neck.



# Principy makroevolučních změn fenotypu: Delece

hadi – jiný mechanismus ztráty předních (homeotická změna identity obratlů) a zadních končetin



**Figure 6.13**  
**Evolutionary transitions in snake limblessness**  
 The phylogeny of snakes indicates that the loss of snake hindlimbs may have evolved once at the base of the snake lineage. The existence of well-developed hindlimbs in the fossils *Pachyrhachis* and *Haasiophis* suggests that hindlimbs reappeared during the evolution of these species, as their ancestor may have been limbless. Alternatively, snake hindlimbs could have been independently lost in each limbless snake lineage.  
 Source: Redrawn from Greene HW, Cundall D. *Science* 2000; 287: 1939–1941.

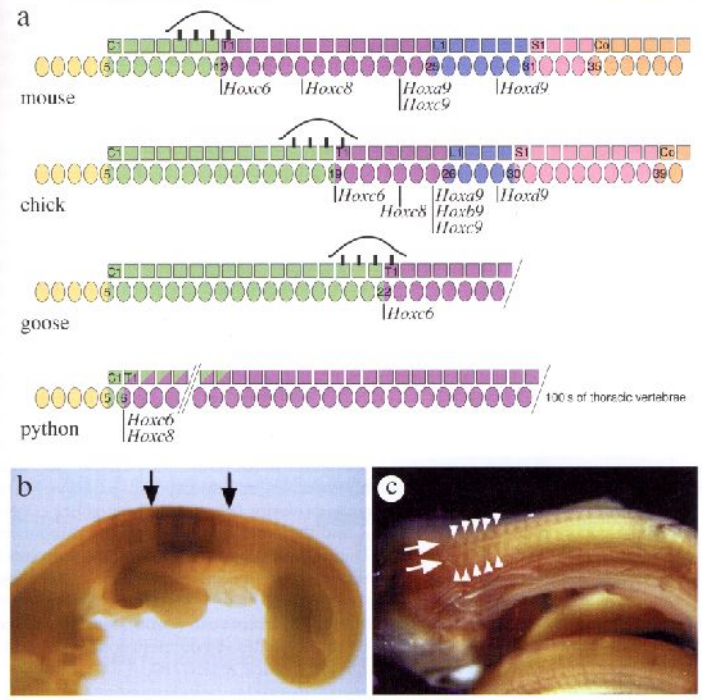


**Figure 5.6**  
**Hox genes and the evolution of tetrapod axial identities**  
 Differences in the axial organization of tetrapods are reflected in shifts in *Hox* gene expression domains between animals. (a) The anterior boundaries of expression of several *Hox* genes in the paraxial mesoderm are shown beneath the somites (circles) and vertebrae (squares) of the mouse, chick, goose, and python body plans. In mammals and birds, which have distinct cervical (green) and thoracic (purple) axial regions, the anterior boundary of the *Hoxc6* gene lies at the cervical–thoracic transition, even though the axial position [somite number] of this transition falls at a different position in each organism. Similarly, the anterior boundary of *Hoxc2* expression lies within the thoracic region of chicks and mice; the *Hoxa2*, *Hoxb2* and *Hoxc5* boundaries lie near the thoracic–lumbar transition, and the *Hoxd2* boundary lies near the lumbar–sacral transition. In the python, the *Hoxc6* and *Hoxc8* genes have a more anterior expression boundary, reflecting the expanded thoracic vertebral identities of the snake body plan. (b) Expression of the mouse *Hoxc9* gene in the thoracic region (the extent of high levels of expression is indicated by arrows). (c) Expression of the snake *Hoxc8* gene extends through the anterior of the axial skeleton (indicated by arrows and arrowheads).  
 Sources: Part a modified from Burke AC, Nelson CE, Morgan BA, Tabin C. *Development* 1995; 121: 333–346; parts b and c from Cohn MJ, Tickle C. *Nature* 1993; 399: 474–479.

# Principy makroevolučních změn fenotypu: Delece

## Integrating micro- and macroevolution of development through the study of horned beetles

AP Moczek

Department of Biology, Indiana University, 915 E. Third Street, Myers Hall 150, Bloomington, IN 47405-7107, USA

Heredity (2006) 97, 168–178

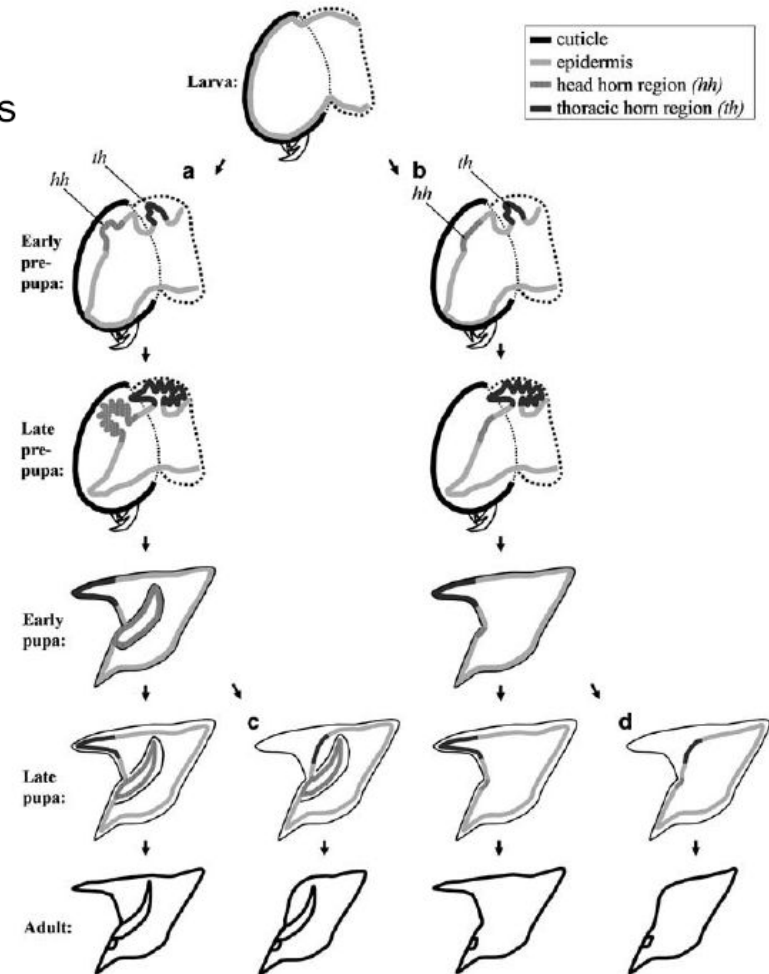
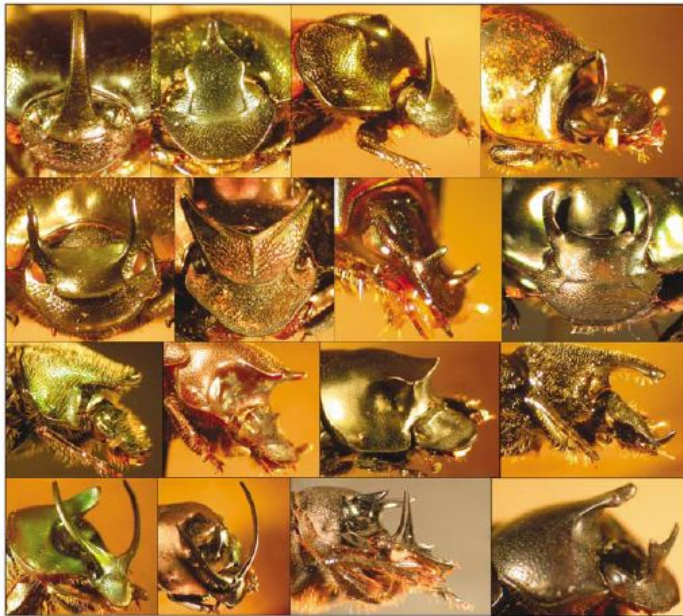


**Figure 2** Development of (a) horns and (b–d) horn dimorphisms in *Onthophagus* beetles. (a) During the last larval instar the larval epidermis (light gray) fully lines the larval cuticle (black). At the onset of the prepupal stage the larval epidermis detaches from the cuticle (apolysis) and selected regions (shown here for a head horn (hh) and thoracic horn (th)) undergo rapid cell proliferation. The resulting extra tissue folds up underneath the larval cuticle. The epidermis subsequently secretes the future pupal cuticle, which upon the molt to the pupal stage forms the outermost layer of the pupa, lined once again by a layer of epidermal cells. During this pupal molt horn primordia are able to expand and unfold, and are now visible externally. During the second half of the pupal stage epidermal cells apolysise once more. This time, however, no significant growth of horn tissue follows apolysis. Instead, epidermal cells secrete one last cuticle and the pupa undergoes one last molt to the final adult stage. (b) Development of horn dimorphisms through differential proliferation of prepupal horn tissue (illustrated here for head horns (hh) only). During the prepupal stage presumptive horn tissue proliferates little or not at all, resulting in the absence of external horns in pupae and the resulting adults. This mechanism is used to generate sexual dimorphisms as well as alternative male morphologies for head horns in many species. (c and d) Development of horn dimorphisms through differential loss of pupal horn tissue (illustrated here for thoracic horns (th) only). Pupal horn epidermis is resorbed prior to the secretion of the final adult cuticle, most likely via programmed cell death. In many cases resorption of pupal horn tissue can completely erase the former presence of a thoracic horn. This mechanism contributes to sexual dimorphisms for thoracic horns in many species, and can occur in the presence or absence of (differential) head horn development.

## Principy makroevolučních změn fenotypu: Heterochronie

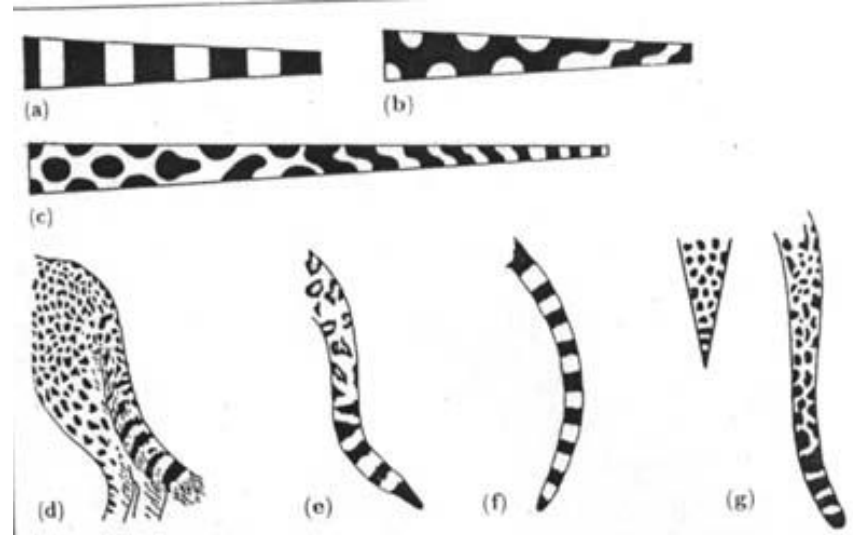
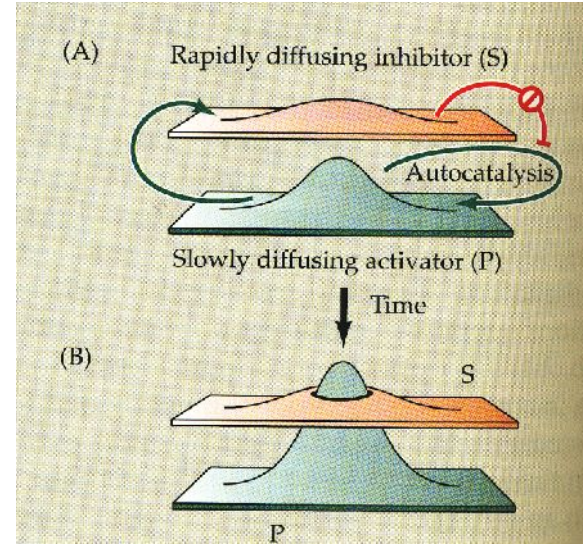


X thyrotropin

# Principy makroevolučních změn fenotypu: Heterochronie



## Turingův oscilátor



# Principy makroevolučních změn fenotypu: Heterochronie

*J. Zool., Lond.* (1994) 232, 633-639

## Ratite-like neoteny induced by neonatal thyroidectomy of European starlings, *Sturnus vulgaris*

A. DAWSON, F. J. McNAUGHTON,

*NERC Institute of Terrestrial Ecology, Monks Wood, Abbots Ripton, Huntingdon PE17 2LS, UK*

A. R. GOLDSMITH

*AFRC Research Group on Photoperiodism & Reproduction, Department of Zoology, University of Bristol, Bristol BS8 1UG, UK*

AND A. A. DEGEN

*Desert Animal Adaptations and Husbandry, Jacob Blaustein Institute for Desert Research, Ben Gurion University of the Negev, P.O. Box 653, Beer-Sheva, Israel*



636

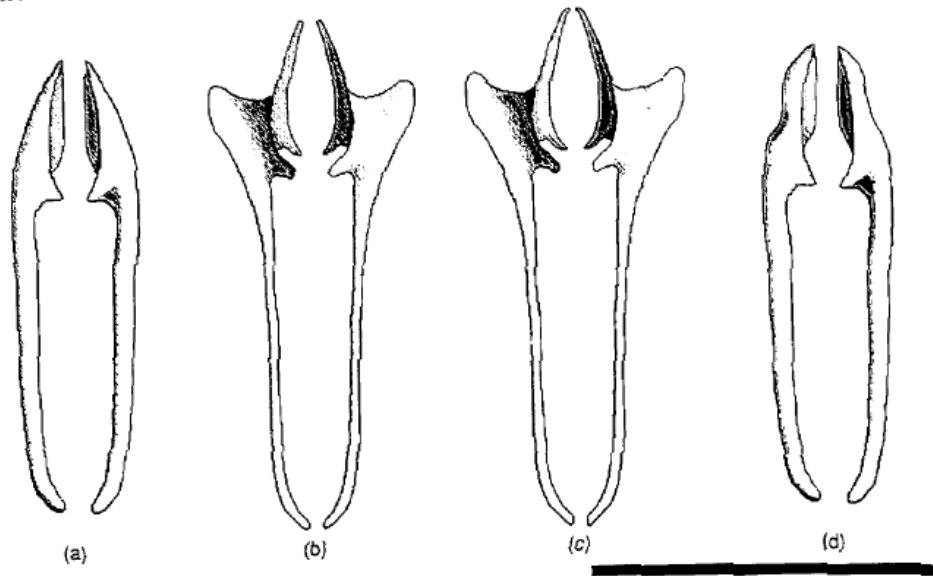
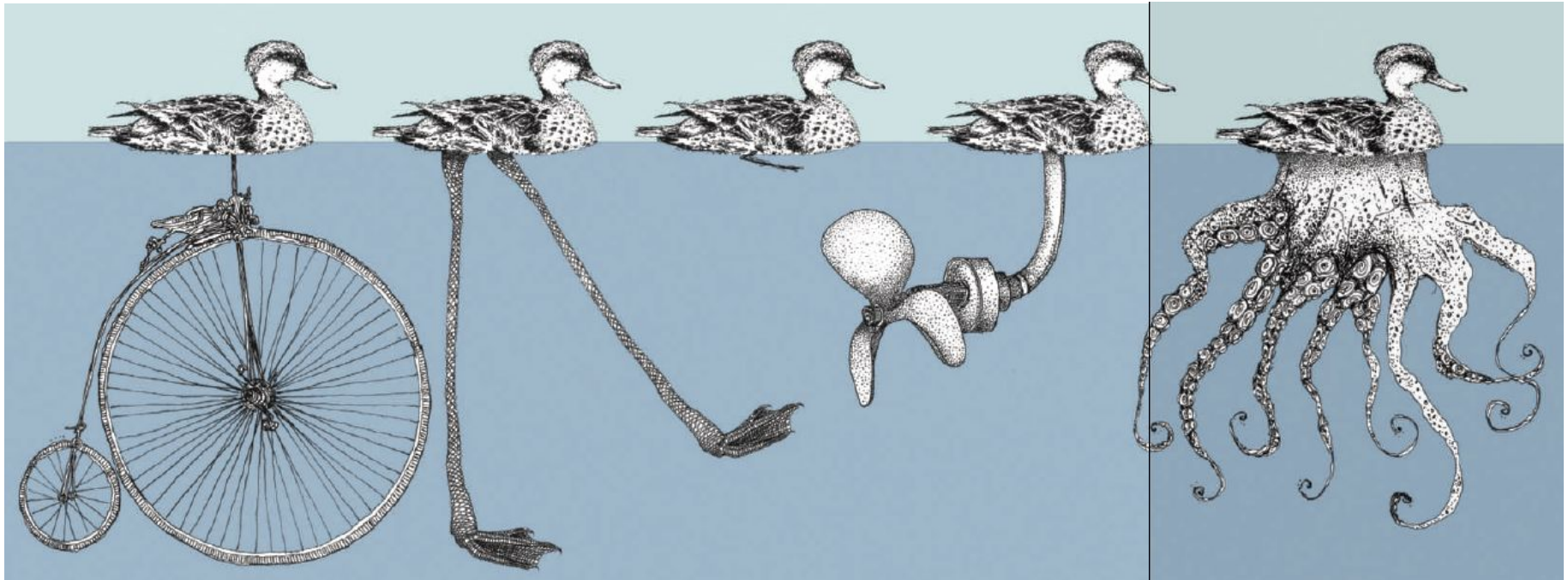


FIG. 2. The ventral aspect of the palatine bones of control starlings at: (a) three weeks; (b) six weeks; and (c) one year old (d) The palatine bones of a one-year-old starling thyroidectomized at eight days of age. In control birds, the bones were fully formed by six weeks of age. In thyroidectomized birds, the bones remained undeveloped, similar to those of euthyroid controls at three weeks of age. The scale bar represents 10 mm.

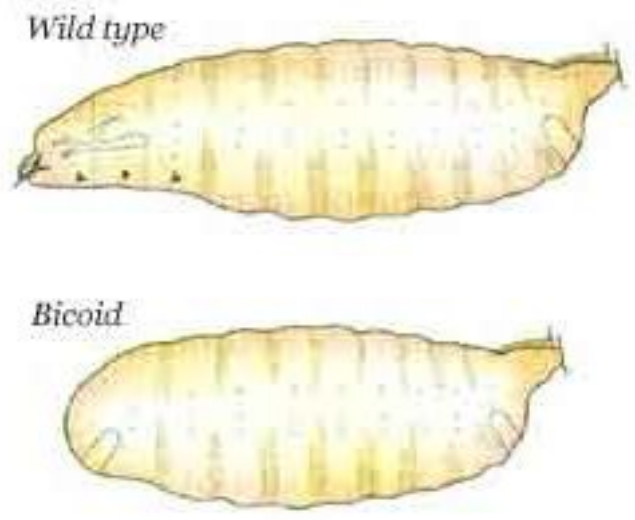
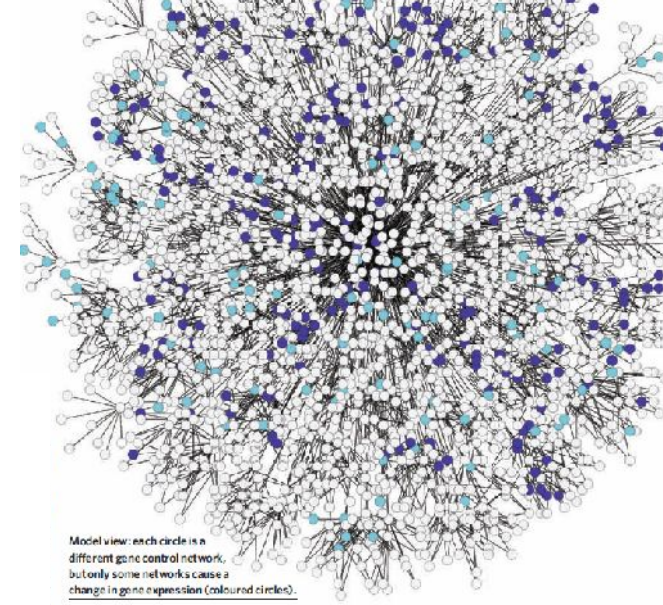
## Konzervatismus fyziologických a vývojových drah?



# Beneath the surface

You might think that once evolution has found one way to get something done, it will stick with it. But similar physical forms can hide radically different wiring, finds **Tanguy Chouard**.

*Bicoid* nezbytný pro octomilku, ale jiný hmyz ho nemá



# Změna kontroly regulační sítě u kvasinek

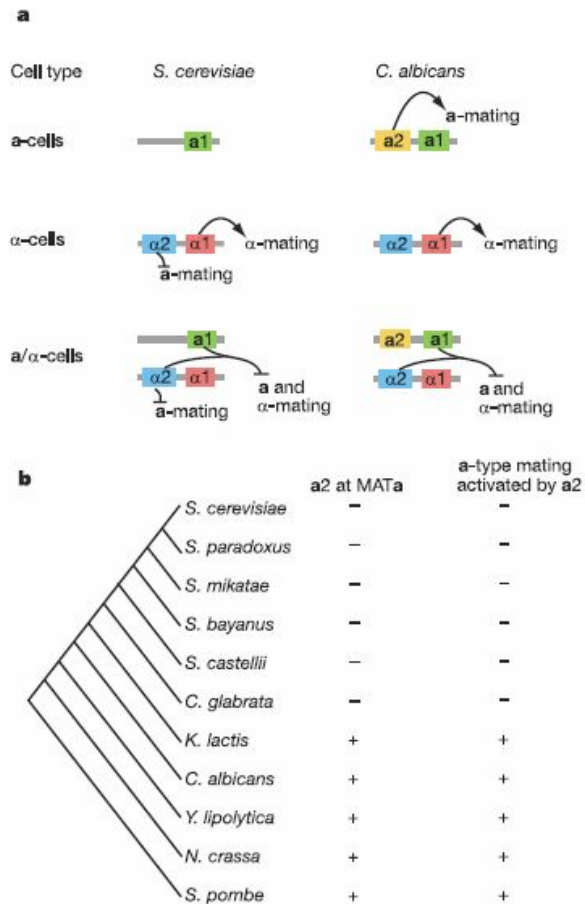


**Figure 1 | a-type mating is negatively regulated in modern *S. cerevisiae*, but was positively regulated in its ancestor.** **a**, *S. cerevisiae* and *C. albicans* transcribe their genes according to one of three programs, which produce the a-,  $\alpha$ - and a/ $\alpha$ -cells. The particular cell type produced is determined by the MAT locus, which encodes sequence-specific DNA-binding proteins (coloured blocks). Regulation of a-type mating differs substantially between *S. cerevisiae* and *C. albicans*. In *S. cerevisiae*, a-type mating is repressed in  $\alpha$ -cells by  $\alpha 2$ . In *C. albicans*, a-type mating is activated in a-cells by a2. In both organisms, a-cells mate with  $\alpha$ -cells to form a/ $\alpha$ -cells, which cannot mate. **b**, a2 is an activator of a-type mating over a broad phylogenetic range of yeasts<sup>16,18–21,47</sup>. In *S. cerevisiae* and close relatives, a2 is missing and  $\alpha 2$  has taken over regulation of the *asgs*<sup>22</sup>.

# Evolution of alternative transcriptional circuits with identical logic

Annie E. Tsong<sup>1,2,†</sup>, Brian B. Tuch<sup>1,2,†</sup>, Hao Li<sup>1</sup> & Alexander D. Johnson<sup>1,2</sup>

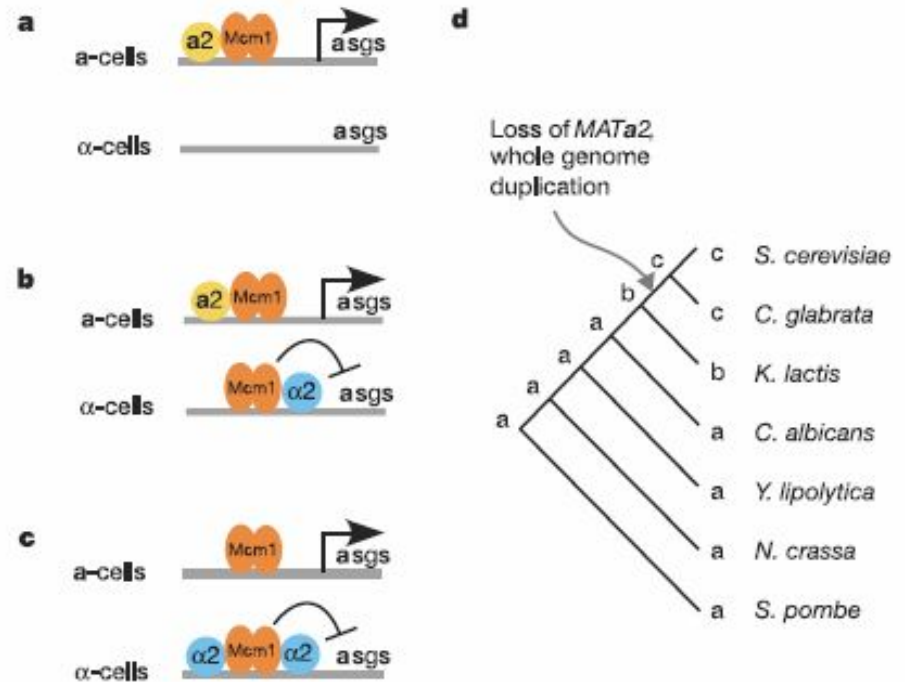
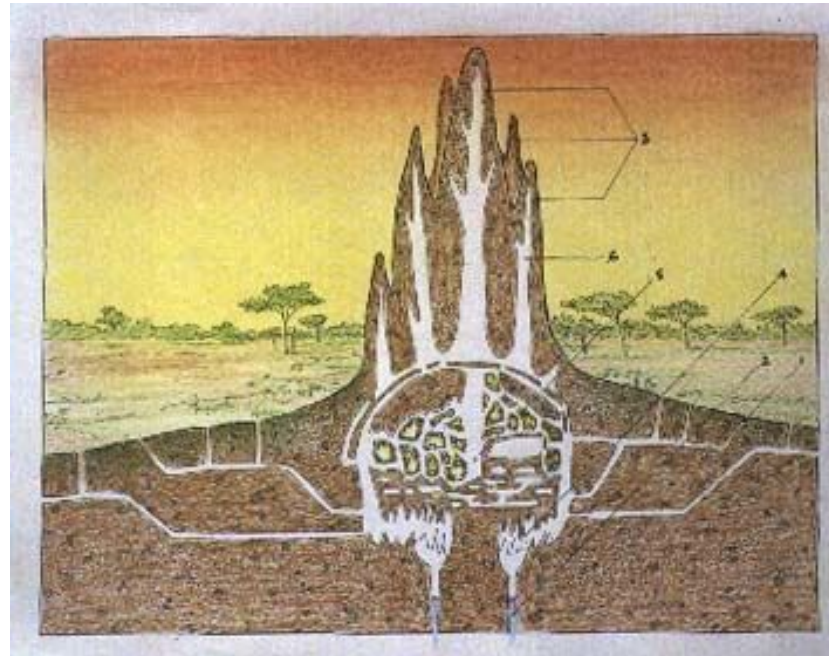
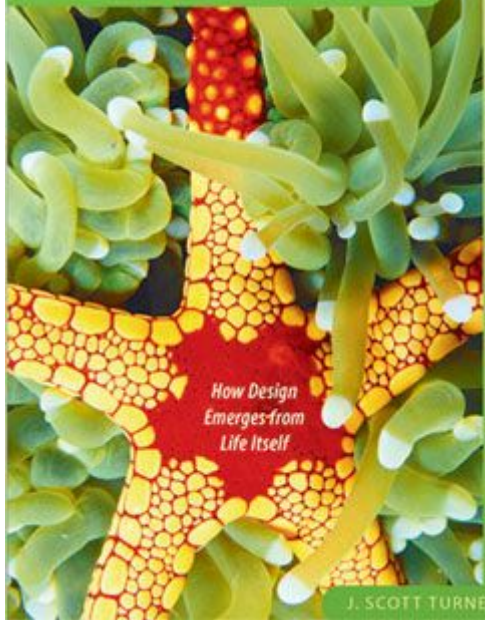


**Figure 6 | Ordering the changes in cis- and trans-regulatory elements.** **a**, In an ancestral yeast, a2–Mcm1 activated *asgs* in a-cells. This scheme persists in modern *C. albicans*. **b**, cis- and trans-elements in the *K. lactis* branch suggest that *asgs* are positively regulated by a2–Mcm1 in a-cells and negatively regulated by  $\alpha 2$ –Mcm1 in  $\alpha$ -cells. **c**, In modern *S. cerevisiae*, *asgs* are activated by Mcm1 in a-cells and repressed by  $\alpha 2$ –Mcm1 in  $\alpha$ -cells. **d**, The regulatory schemes shown in **a–c** are mapped onto extant species and ancestral nodes. Species from *C. albicans* to *S. pombe* most closely resemble **a**<sup>16–19</sup>, whereas *K. lactis* fits **b** and *S. cerevisiae* and *C. glabrata* fit **c**. The most parsimonious evolutionary scenario maps scheme **a** as the ancestral state. Scheme **b** is transitional, first appearing in the ancestor of *K. lactis* and *S. cerevisiae*. Scheme **c** is the most derived, appearing in the ancestor of *C. glabrata* and *S. cerevisiae*.



THE TINKERER'S ACCOMPLICE



?

Zkouška:

- po domluvě ([lukkrat@email.cz](mailto:lukkrat@email.cz), případně mobil 608380581)